A Data-Driven Approach To Design And Control Of Underwater Vehicle Propulsor Inspired By Black Ghost Fish

Arash Taheri

Division of Applied Computational Fluid Dynamics, Biomimetic and Bionic Design Group, Tehran, Iran
(Corresponding Author: taha.bionics@gmail.com)

Abstract: *In this paper, a design methodology for a ribbon-fin propulsor inspired by electric black ghost knifefish is introduced based on the machine learning concept. In this regard, an artificial multi-layer perceptron neural network (MLPR) is designed and trained based on the available experimental data. Afterward, the proposed MLPR is coupled with an evolutionary optimization technique, i.e. breeder genetic algorithm (BGA), towards an optimum design strategy. The results show the robustness and effectiveness of the introduced approach to design and control of this kind of bio-inspired propulsion systems. The outcome of the study also demonstrates capability of the proposed approach to provide a deeper insight into the design hyperspace, via generalization of the experimental data.*

Keywords: *Bio-propulsion, Black Ghost Fish, Underwater Robotics, MLPR, BGA, Bionics*

I. INTRODUCTION

Flexibility and deflection dynamics of the body, tails and fins of aquatic swimming animals provided by natural soft bio-materials is the underlying physical principle adopted in the aquatic environment for bio-propulsion generation [1, 2]. This fundamental concept is observed in fishes with different modes of body-tail and fin oscillation/undulations, jellyfish with a deformable bell and flexible tentacles and cephalopods such as a squid or octopus with a jet propulsion, to name a few [1]. For instance, cyclic bell deformations and tentacle deflection dynamics in the medusan swimming, determine locomotion and propulsion generation of the aquatic animal [3]-[6]. Another important factor that majorly contributes in the swimming and locomotion performance of the aquatic animal is the external morphology (eidonomy) of the marine creatures [1]. In short, aquatic animal's eidonomy by itself or via a nonlinear interplay with the body deflection dynamics governs essential features encountered in the swimming process, such as: vortex generation and dynamics, onset and development of separation on the animal's body, flow attachments and detachments, to name a few [7]-[13]. In general, fish locomotion can be classified based on the different swimming modes. For anguilliform swimmers, a relatively large portion of the body undulates to generate bio-propulsion, whereas in the case of carangiform swimmers a smaller portion of the body, e.g. about half of the body length, oscillates. In the ostraciiform swimming mode, fish's tail oscillates. There is another group of swimmers, namely gymnotiform, involving interesting species such as black ghost knifefish, *Apteronotus albifrons* with a ventral ribbon-fin propulsor (Fig. 1) and Africa weakly electric fish, *Gymnarchus Niloticus*, with a dorsal ribbon-fin propulsor, to name a few. For these swimmers, body can be considered rigid and propulsion is majorly produced by undulation of a ribbon-fin along the body; in other words, it can be assumed that (body deformation ☐ fin deformation).

Black ghost knifefish is an agile fish, which belongs to the weakly electric fish group and exhibits impressive maneuvering capabilities in the aquatic environments. In general, a strongly electric fish can adopt electric field generation to kill or damage the prey or repel enemies, whereas a weakly electric fish adopts the electric field for navigation or recognizing the prey, electro-location and electro-communications [14, 15]. In this regard, black ghost knifefish utilizes Electric Organ Discharge (EOD) to generate electric fields in the surrounding environment using a so-called 'electric organ' at the end of the body or the tail (Fig. 1). In the electro-sensory process, a weak electric field is continuously generated by EOD around the knifefish. Thanks to the relative rigidity of the body in the gymnotiform swimming mode (i.e. body deformation ☐ fin deformation), the electric field generated by the wave-type EOD for a knifefish is not perturbed apriori by repetitive oscillations or undulations of the body (unlike anguilliform, carangiform and ostraciiform swimming modes). Therefore, the ribbon-fin propulsion system makes it possible for a black ghost fish to keep the body relatively rigid and in this way facilitates the electro-sensory performance. In the next step, by entering an object into the electric field, the electric field is perturbed and ultimately the object is detected (seen) by several thousands of

---

electro-receptors (sensors) on the body surface of a knifefish [15]. The knifefish can reach a maximum length of 50 cm and can effectively swim by sending undulatory traveling waves along the ribbon-fin in the forward and backward directions. This interesting mechanism gives the ability of very fast reverse movements (in 100 ms) without turning, just by changing the direction of the traveling waves [16]. In fact, a black ghost fish can impressively swim in the backward direction as fast as in the forward direction [17]. This type of propulsion system can also provide a rapid acceleration and is highly efficient for transportation at low Reynolds number flow regimes [17]. As observed by Julian et al., gymnotiform swimmers possess half of the oxygen consumption compared to the non-gymnotiform swimmers, which proves great efficiency of this type of the bio-propulsion systems [18]. It is also interesting to mention that according to a recent research [19], a knifefish is capable to generate a powerful suction in the feeding process, generating a strong acceleration equals to 450 g , where g is the acceleration of gravity. This large amount of force can lead to a maximum chance for prey capturing and also can cause a serious physical damage on the prey before its capturing and in this way facilitates hunting [19]. In the next section, hydrodynamics of the knifefish bio-propulsion system is briefly discussed.
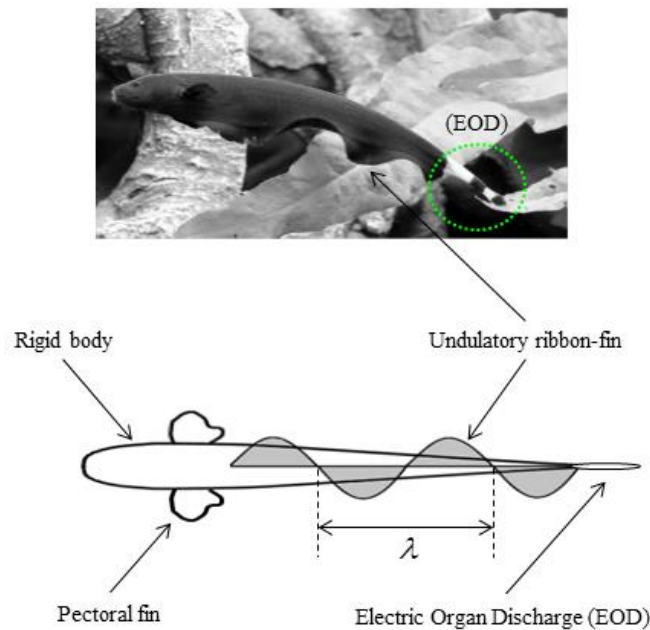
Figure 1. Black ghost knifefish (*Apteronotus albifrons*); (top) knifefish swimming with ribbon-fin propulsion [20], (bottom) schematic of the knifefish bio-propulsion system using travelling waves along the fin

II.   BLACK GHOST KNIFEFISH HYDRODYNAMICS & BIO-PROPULSION

As abovementioned, a knifefish swims in the forward and backward directions by the aid of an efficient propulsor based on the ribbon-fin undulations. Vortex ring-induced propulsion is the key concept to explain thrust generation by a ribbon-fin. In fact, a vortex ring in the flow field induces a local jet at its centerline, which can be simply expressed by the following equation:

$$\nabla^2 \vec{u} = -\nabla \times \vec{\omega} \tag{1}$$

where $\vec{u}$ and $\vec{\omega}$ denotes fluid velocity and vorticity vectors, respectively. In this sense, a vortex ring can be viewed as mechanism that can impart momentum into the fluid flow. As clarified by the aid of Computational Fluid Dynamic (CFD) simulations based on the Immersed Boundary (IB) method, ribbon-fin undulations at an intermediate Reynolds number, i.e. 10^3-10^4, create a 'crab-shaped' system of vortex rings along the ribbon [21, 22]. This complex vortical system is capable to generate a powerful propelling streamwise jet, which in turn create thrust according to the Newton's 3rd law. Furthermore as shown by Shirgaonkar et al., generation of two counter-rotating axial vortex pairs attached to the ribbon-fin tip is responsible for heave force generation adopted by the aquatic animal for station keeping [21, 22]. This propulsion system is also capable to produce off-axis thrust [23] and to provide a proper level of maneuverability for the black ghost knifefish [24].

III.   DATA-DRIVEN DESIGN APPROACH BASED ON MACHINE LEARNING CONCEPT

A simplified model of the ribbon-fin of a knifefish can be materialized as a narrow rectangle sheet with a height and longitudinal length equals to h and L , respectively. As one can see in Fig. 1, undulations of the ribbon-fine can be idealized by a 'sinusoid' function. Mathematically, the deflection angle between the ribbon-

fin sheet and the vertical symmetry-plane of the fish body can be expressed at any longitudinal position along the fin in terms of time, as below [25]-[27]:

$$\theta(x,t) = \theta_{max} \sin\left(2\pi\left\{\frac{x}{\lambda} - f \times t\right\}\right) \tag{2}$$

where θ_{max} is the maximum angular deflection of the sheet during the oscillations. Parameters f and λ is the frequency and wave length of undulations, respectively. Variable x also denotes the coordinate in the axial (longitudinal) direction along the fin and t stands for time. The longitudinal thrust force of a freely swimming ribbon-fin can be expressed as below:

$$Thrust = T_r = \Psi\left(\text{Re}, h^\dagger, \lambda^\dagger, f, \theta_{max}\right) \tag{3}$$

where Re is the Reynolds number and is defined as $\text{Re} = u_c L_c / v$, where u_c, L_c and v is a characteristic velocity, characteristic length and kinematic viscosity, respectively . In the equation, the parameter $\lambda^\dagger$ stands for the non-dimensional wave length and is defined as $\lambda^\dagger = \lambda / L$. The parameter $h^\dagger$ is the ribbon-fin aspect-ratio and is defined as $h^\dagger = h / L$. In the present paper, the idea is to utilize machine learning concept with the aid of an artificial neural network (ANN) trained with available data sets, either from experiments or CFD simulations, to model the Ψ function. In general, ANN is one of the well-fitted methods for generalization of data in systems with non-linear dynamics and/or missing data. Its concept is based on the brain functionality and how brain learns. In fact, ANN mathematically mimics the brain learning process via a non-linear modeling of neurons and theirs synaptic inter-connections. In this study, a feed-forward MLPR with the architecture (5-20-1) is designed to model ribbon-fin thrust as shown in Fig. 2. The net consists of an input layer with 5 non-linear neurons corresponding to 5 input parameters, including: Re, $h^\dagger$, $\lambda^\dagger$, f and θ_{max}. The output layer has only a single neuron corresponding to the thrust of the ribbon-fin propulsor. There is only one hidden layer in the architecture, possessing 20 neurons here. It is also straight-forward to add another hidden layer to increase the capability of the MLPR with an architecture as (5-$\Re$-$\Im$-1), where $\Re$ and $\Im$ is the number of neurons in the first and second hidden layers, respectively; which can be optimized based on the size of the data set. The latter architecture is recommended in the case of large training data sets with high degree of non-linearity.
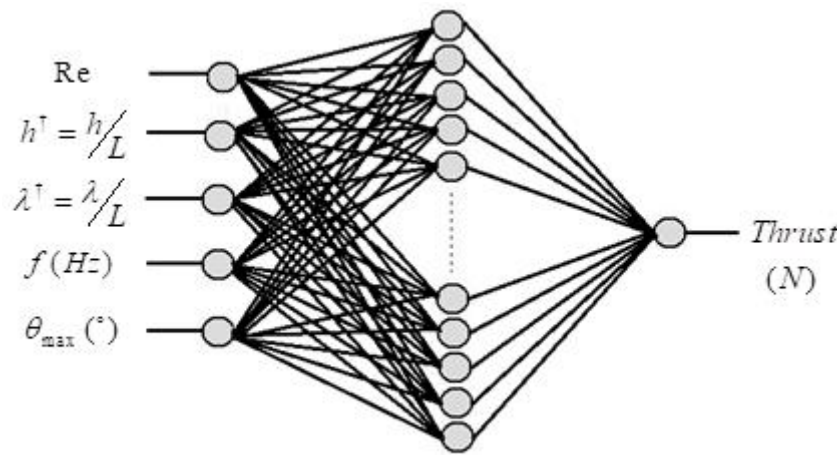
Figure 2. MLPR architecture (5-20-1) adopted for the knifefish propulsion (Ψ) modeling

The neuron is a simplified mathematical model of a real neuron in biological sciences. The nonlinear model of a neuron can be illustrated as seen in Fig. 3. In fact, for a single neuron, the weighted summation of input signals is accumulated and a bias (threshold) term is also added, the resultant is then fed into an activation function and ultimately the output signal is obtained. In mathematical term, it can be stated as below [28, 29]:

$$y_i^p = \varphi_{ANN}(v_i^p) = \varphi_{ANN}(\sum_{j=1}^{N} w_{i,j}^p x_j^p + b_i^p) \tag{4}$$

where v_i^p and y_i^p is the activation potential and neuron output signal, respectively. Neurons in a typical MLPR are organized in several distinct layers, namely input, output and hidden layers and are inter-connected to each other via distinct synaptic weights in inter-connections of the layers, as shown in Fig. 2.
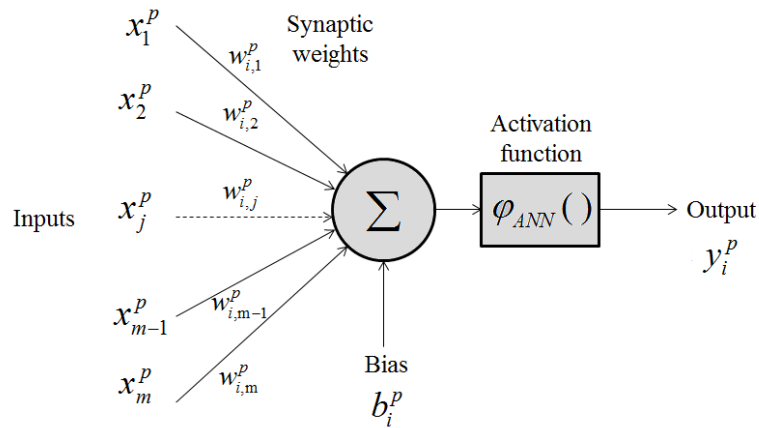
Figure 3. Nonlinear model of a biological neuron (synaptic weights, bias and activation function)

In the learning process, signals are passed in two distinct opposite directions, namely 'forward' and 'backward' directions. In the forward direction governed by equation (4), the input signals passing via the inter-connections are weighted and added to the bias and the result coming from the activation function is transmitted to the next layer. Mathematically, net output of neuron i in layer $s+1$ can be written as below:

$$y_i^{s+1} = \varphi_{ANN}^{s+1}(v_i^{s+1}) = \varphi_{ANN}^{s+1}(\sum_{j=1}^{N} w_{i,j}^{s+1} x_j^s + b_i^{s+1}) \tag{5}$$

In the forward propagation of the signal all synaptic weights are considered 'fixed' values come from the previous iteration. At the output-layer, the difference between the output signals and target signals are computed and a cost function or error is defined as a norm of this difference. Then, the backward propagation phase begins. In this phase, synaptic weights of the ANN are adjusted using a so-called 'delta learning rule' in a way to minimize the error. This process is so-called 'learning' of a neural network. Mathematically, the MLPR output deviation signal for neuron i at output layer and at iteration number n is defined as the following:

$$\varepsilon_{ANN}^n(w_{i,j}) = \frac{1}{2}\sum_{i=1}^{N_O}[y_i(n) - T_i(n)]^2 \tag{6}$$

where N_O denotes the number of ANN outputs. Furthermore, T is the target vector for the neural network. The goal is to minimize the deviation between the ANN output and the target values. In the delta learning rule, synaptic weights are adjusted based on the steepest descent method in the backward propagation, as below [28]:

$$w_{i,j}^{new} = w_{i,j}^{old} - \eta_L \frac{\partial \varepsilon_{ANN}^n}{\partial w_{i,j}} \tag{7}$$

where η_L is the 'learning rate' of the MLPR. The above relation can be rewritten with local gradient ς_i^{s+1}, as the following:

$$w_{i,j}^{new} = w_{i,j}^{old} - \eta_l \sum_i \varsigma_i^{s+1}(n) y_i^s(n) \tag{8}$$

where the local gradient can be calculated for the hidden layers as below:

$$\varsigma_i^{s+1}(n) = \varphi_{i,ANN}'^{s+1}(v_i^{s+1}(n))\sum_k \varsigma_k^{s+2}(n) w_{k,i}^{s+2}(n) \tag{9}$$

where for the output layer, the gradient is as the following:

$$\varsigma_i^{s+1}(n) = \varphi_{i,ANN}'^{s+1}(v_i^{s+1}(n))[y_i^{s+1}(n) - T_i^{s+1}(n)] \tag{10}$$

In general, shape of the activation function can be selected among continuous and differentiable functions. Learning rate, η_L, is another important parameter, which determines the rate of change of synaptic weights at each iteration. This parameter resembles a 'relaxation factor' typically utilized in the discretization schemes for solving PDEs in CFD applications. By lowering η_L, ANN convergence rate typically decreases, although it can lead to a smoother trajectory path in the ANN 'weight-space', provided by the steepest descent method. As a result, lowering the learning rate reduces the risk of divergence in the learning process.

In the present paper, for the training phase of the designed MLPR (5-20-1), an experimental data set for the ribbon-fin propulsion obtained by Epstein et al. is adopted [25]-[27]. The experiments were performed on a ribbon fin with a height h and length L equals to 7.62 cm and 23.114 cm, respectively. In the experiment, Re and $h^\dagger = h/L$ is considered constant and approximately equals to 7.5×10^3 and 0.33, respectively. The tests were performed for two or three trials for each of 6^3 (i.e. 216) total combinations of the variable parameters adopted in the ribbon-fin propulsion experiment, i.e. $\{\lambda^\dagger, f, \theta_{max}\}$, as the following [25]-[27]:

$$0.7 \le \lambda^\dagger \le 4.2, \ \Delta\lambda^\dagger = 0.7$$
$$0.5\,Hz \le f \le 3.0\,Hz, \ \Delta f = 0.5 Hz \quad (11)$$
$$10^\circ \le \theta_{max} \le 35^\circ, \ \Delta\theta_{max} = 5^\circ$$

After the training phase, the MLPR-ANN learns the non-linear relation between the output, i.e. thrust of the ribbon-fin propulsion T_r, and the inputs, i.e. $\{Re, h^\dagger, \lambda^\dagger, f, \theta_{max}\}$. The outcomes of the learning process are frozen and stored in the adjusted weight and bias matrices. The proposed ANN-model predictions can be utilized for the propulsor design and its control. In this regard, the thrust estimation (MLPR output, i.e. T_r) can be simply and efficiently performed by some matrix manipulations after the training process. Learning history curves of the proposed MLPR during the training phase in stable and unstable regions are shown in Fig. 4.
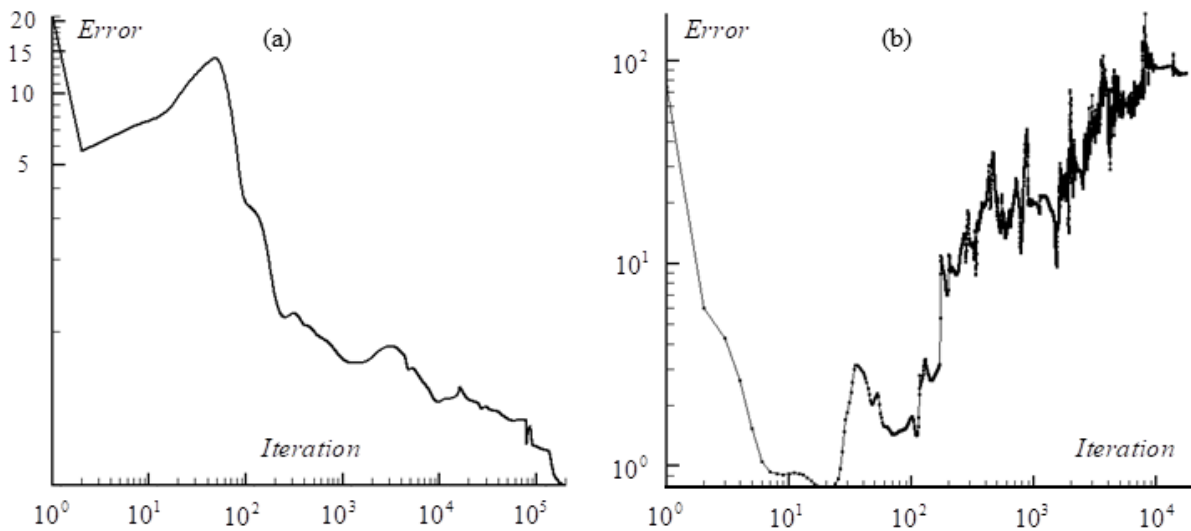
Figure 4. Learning convergence history of the adopted MLPR for the knifefish ribbon-fin bio-propulsion for different learning rates: a) stable region, $\eta_L = 0.02$, b) unstable region, $\eta_L = 0.128$

As one can see in Fig. 4, by applying a learning rate equals to 0.02 as selected here, the error or cost function, i.e. equation (6), effectively decreases to a value lower than 5×10^{-3} (Fig. 4- part (a)), while for a learning rate greater than 0.128, the learning process diverges (Fig. 4- part (b)). In the training phase, 90% of the experimental data set was used for the training purposes and 10% was kept for the validation process. As an example, Fig. 5 depicts a comparison between the ANN predictions and the experimental data. As one can see in the figure, the MLPR meta-model predictions are in a close agreement with the experiment. This verifies the ability of the proposed strategy for appropriate predictions of the knifefish-inspired propulsor performance using design parameters as inputs, including: Re, $h^\dagger$, $\lambda^\dagger$, f and θ_{max}. As a result, the trained ANN can be utilized as a fast estimation tool to predict thrust of this kind of bio-inspired ribbon-fin propulsions in the preliminary design phase. Furthermore, it can be also used in the core of a controller unit of a knifefish-inspired propulsor to adjust the parameters accordingly. As mentioned before, this is simply done by performing computationally efficient matrix multiplications/manipulations. Furthermore, the proposed MLPR set-up lets a designer to add future experimental data by simply adding new data to the database with no restriction and no additional modifications. In this way, accuracy of the trained MLPR predictions increases specially on the parameters with more available experimental data. For example, for the meta-model here, more data with Re and $h^\dagger$ variations is needed, either from the experiments or CFD simulations to increase the accuracy of the ANN model predictions in a wider range of the design parameters. In general, the ANN output can be interpreted as a 3D

hyper-surface in a 4D design-space. Because it is not possible to illustrate a 4D design-space on a sheet of paper, therefore three distinct graphs of the mutual variations of the thrust force (T_r) versus two variables (out of three variables, i.e. $\lambda^\dagger$, f, θ_{max}) are shown in Fig. 6. As one can see in the figure, there is a smooth and continuous variation for the meta-model predictions as 2D curved surfaces illustrated in 3D. All of the 2D response surfaces (defined by constant values of $\lambda^\dagger$, f or θ_{max}) have its own extremum region/point (maximum thrust), shown by red color in Fig. 6. Global optimization of the knifefish-inspired propulsor is presented in the next section.
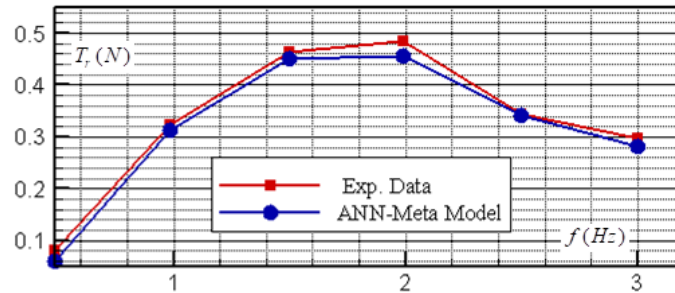
Figure 5 Propulsor thrust prediction by the proposed meta-model (ANN) compared with the experimental curve in terms of the frequency of the ribbon-fin undulations for $\theta_{max} = 35$ and $\lambda^\dagger = 2.8$
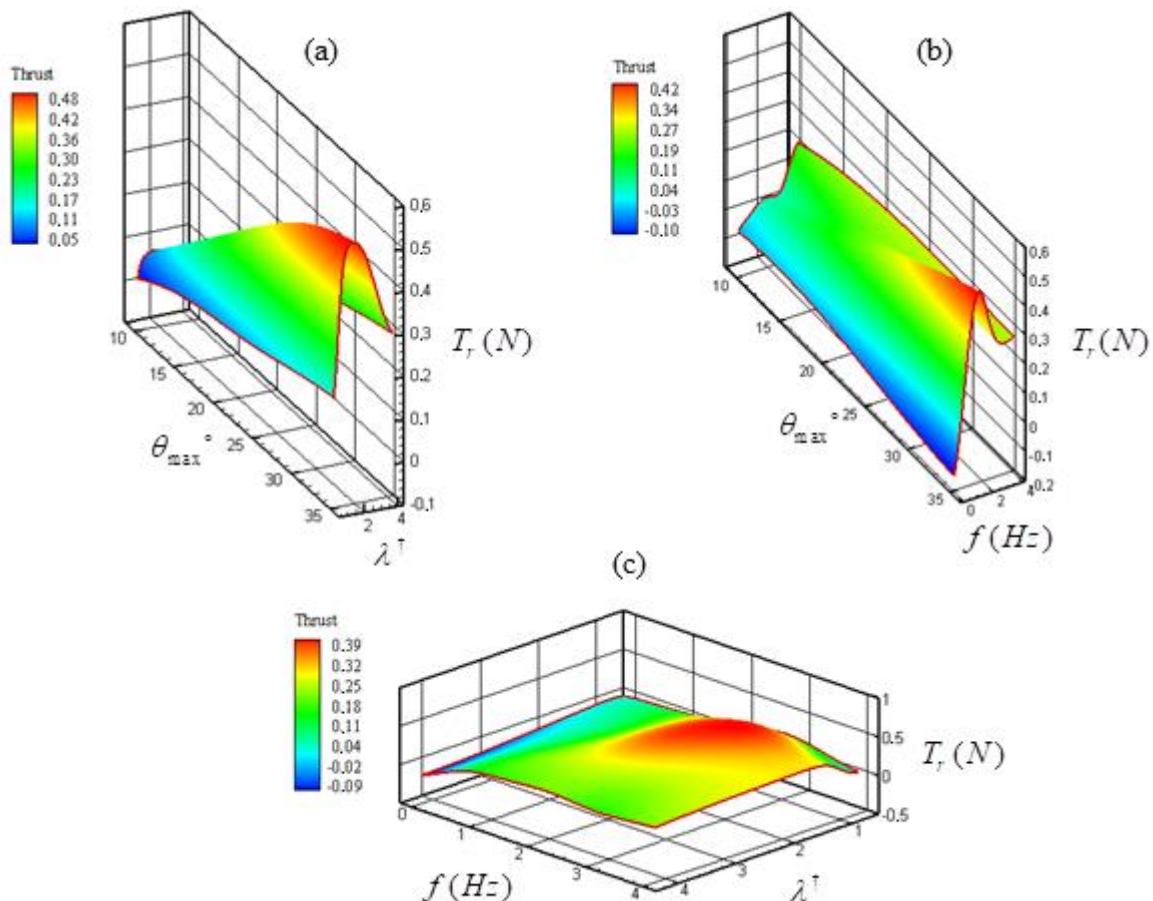
Figure 6. Design hyper-space morphology; the meta-model ANN predictions for the knifefish ribbon-fin bio-propulsion: a) thrust T_r versus θ_{max} and $\lambda^\dagger$ with applying $f = 2.0$, b) thrust T_r versus θ_{max} and f with applying $\lambda^\dagger = 3.0$, c) thrust T_r versus f and $\lambda^\dagger$ with applying $\theta_{max} = 25$

IV. DESIGN OPTIMIZATION USING BREEDER GENETIC ALGORITHM

Having on hand, all weights and bias of the trained MLPR in a matrix format, a fitness function typically utilized in optimization techniques can be efficiently evaluated. In this research, for optimization of the knifefish-inspired ribbon-fin propulsor, Breeder Generic Algorithm (BGA) as an evolutionary optimization method is adopted, due to the continuous nature of the problem variables here [30]-[33]. In general, Genetic Algorithms (GA) mimic natural biological evolution based on the principle of survival of the fittest species [30]-[33]. In the technique, a fitness function defined based on given variables is maximized/ minimized. In general, BGA like other GA approaches is an efficient optimization method, inspired by the concept of evolution of species and natural selection, however the population evolution is 'driven' here by 'breeding mechanism' inspired from biology [30]-[33]. Mathematically, for two parents of real numbers $\{\varphi_i\}$ and $\{\zeta_i\}$, a discrete recombination operator is defined similar to the 'crossover' operator in GA, as below [30]-[33]:

$$\xi_i = \varphi_i + \gamma.(\zeta_i - \varphi_i) \tag{12}$$

where γ is a random variable with a uniform distribution in the interval $[-\tau, 1+\tau]$, where τ is set in the interval [0,0.5], here $\gamma = 0.5$. On the other hand, a continuous 'mutation operator' is defined as below [30]-[33]:

$$\varphi_i = \varphi_i \pm \overline{\Delta}_i.2^{-(\sigma.\varepsilon)}$$
$$\overline{\Delta}_i = \upsilon\Delta_i, \ \upsilon \in [0.1, 0.5] \tag{13}$$

where σ is the precision of the machine that optimization is performed on, while ε is a random number selected between integer values 0 and 1. Furthermore, Δ_i is the interval of the variable φ_i. Other steps of the BGA optimization procedure, such as: initialization, fitness evaluations, selection and iterations are the same as the ordinary GA [30]-[33]. In this section, the BGA procedure, as described above, is used to specify an optimum propulsor setting to achieve the maximum available thrust based on the training data set. As mentioned before, for estimation of thrust of the knifefish propulsion, the meta-model is used. For the problem here, the goal of the optimization process is to obtain the parameter setting to get maximum thrust, so the fitness value is considered equal to the thrust. The fitness convergence history curve of the optimization problem is shown in Fig. 7. The optimum combination of parameters is achieved as follows:

$$\{\lambda^{\dagger}, f, \theta_{max}\} = \{2.33, 1.73, 39.78\} \tag{14}$$

The above parameter setting was obtained with an unconstrained optimization approach. That is why θ_{max} can exceed the maximum value of the angular deflection of the ribbon-fin sheet of the propulsor for the maximum achievable thrust. The method is also capable to consider constraints in the optimization process.
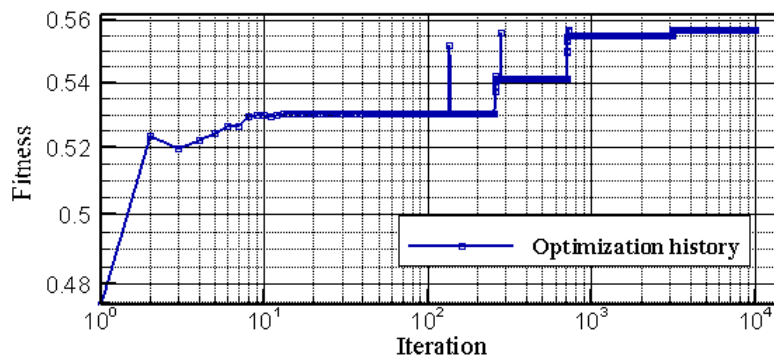
Figure 7. BGA convergence history for an unconstrained optimization of the knifefish-inspired propulsor

V. CONCLUSION

In this paper, a design methodology was proposed based on the machine learning concept coupled with an optimization approach towards an optimum design setting for a bio-inspired ribbon-fin propulsion system. To reach the goals of the paper, the bio-inspired ribbon-fin propulsion was modeled numerically using a MLPR meta-model with one hidden layer and trained using experimental data. The effects of propulsive wave variable variations on the thrust generation of the propulsion system were also studied. In fact, the ANN generalized the experimental results to obtain a model for the ribbon-fin dynamics. The results depict an excellent accuracy of the proposed meta-model. As a result, the trained ANN can be used as a quick estimation tool for the ribbon-fin thrust values at the preliminary design phase with low computational effort compared to CFD solvers that are much more time-consuming. Furthermore, the meta-model can provide a reliable environment in the design

hyper-space to explore the ribbon-fin behaviour in details. In addition, the proposed model was coupled successfully with BGA to achieve an optimum parameter setting for the maximum thrust status. The method is capable to easily consider any technological or general limitations as constraints in the numerical procedure.

Acknowledgements

REFERENCES

[1] A. Taheri, Fluid Dynamics And Bio-Propulsion Of Animal Swimming In Nature: Bionics (Tehran: Arshadan Publication, 2021).
[2] K.N. Lucas, N. Johnson, W.T. Beaulieu, E. Cathcart, G. Tirrell, S.P. Colin, B. J. Gemmell, J. O. Dabiri, And John H. Costello, Bending Rules For Animal Propulsion, Journal Of Nature Communications, 5(3293), 2014, 1-7, Doi: 10.1038/Ncomms4293.
[3] A. Taheri, Lagrangian Coherent Structure Analysis Of Jellyfish Swimming Using Immersed Boundary Fsi Simulations, Journal Of Mechanical And Civil Engineering, 15(1), 2018, 69-74.
[4] J.G. Miles And N.A. Battista, Naut Your Everyday Jellyfish Model: Exploring How Tentacles And Oral Arms Impact Locomotion. Fluids Journal, 4(169), 2019, 1-43.
[5] A.P. Hoover, B.E. Griffth And L.A. Miller, Quantifying Performance In The Medusan Mechanospace With An Actively Swimming Three-Dimensional Jellyfish Model, Journal Of Fluid Mechanics, 813, 2017, 1112-1155.
[6] A.P. Hoover And L.A. Miller, A Numerical Study Of The Benefits Of Driving Jellyfish Bells At Their Natural Frequency, Journal Of Theoretical Biology, 374, 2015, 13-25.
[7] A. Taheri, On The Hydrodynamic Effects Of Humpback Whale's Ventral Pleats, American Journal Of Fluid Dynamics, 8(2), 2018, 47-62.
[8] A. Taheri, A Meta-Model For Tubercle Design Of Wing Planforms Inspired By Humpback Whale Flippers, International Journal Of Aerospace And Mechanical Engineering, 12(3), 2018, 315-328.
[9] A. Taheri, Hydrodynamic Impacts Of Prominent Longitudinal Ridges On The 'Whale Shark' Swimming, Research In Zoology, 10(1), 2020, 18-30.
[10] A. Taheri, Hydrodynamic Analysis Of Bionic Chimerical Wing Planforms Inspired By Manta Ray Eidonomy, Indonesian Journal Of Engineering And Science, 2(3), 2021, 11-28.
[11] A. Taheri, Lagrangian Flow Skeletons Captured In The Wake Of A Swimming Nematode C. Elegans Using An Immersed Boundary Fluid-Structure Interaction Approach, International Journal Of Bioengineering And Life Sciences, 15(7), 2021, 71-78.
[12] A. Taheri, On The Hydrodynamic Effects Of The Eidonomy Of The Hammerhead Shark's Cephalofoil In The Eye Bulb Region: Winglet-Like Behaviour, International Journal Of Marine Science And Technology Bulletin, 11(1), 2022, 41-51.
[13] A. Taheri, Topology Of Reverse Von-Kármán Vortex Street In The Wake Of A Swimming Whale Shark, International Journal Of Mechanical And Mechatronics Engineering, 17(8), 2023, 312-318.
[14] P. Moller, Electric Fishes: History And Behavior (London: Chapman & Hall, 1995).
[15] M.E. Nelson, Electrosensory Signal Processing Lab Documentation, Beckman Institute, Neuroscience Research Center, University Of Illinois, Urbana-Champaign, Usa, 2011.
[16] M.A. Maciver, The Computational Neuroethology Of Weakly Electric Fish: Body Modeling, Motion Analysis, And Sensory Signal Estimation, Doctoral Diss., University Of Illinois, Urbana-Champaign, Illinois, 2001.
[17] R.W. Blake, Swimming In The Electric Eels And Knifefishes. Canadian Journal Of Zoology, 61, 1983, 1432–1441.
[18] D. Julian, W.G.R. Crampton, S.E. Wohlgemuth And J.S. Albert, Oxygen Consumption In Weakly Electric Neotropical Fishes, Journal Of Oecologia, 137: 2003, 502-511.
[19] V.M. Ortega-Jimenez And C.P.J. Sanford, Knifefish's Suction Makes Water Boil, Nature Journal-Scientific Reports, 10:18698, 2020, 1-5.
[20] Photo From The Website: Www.Ratemyfishtank.Com, Accessed On 20 August 2023.
[21] A.A. Shirgaonkar, O.M. Curet, N.A. Patankar And M.A. Maciver, The Hydrodynamics Of Ribbon-Fin Propulsion During Impulsive Motion, Journal Of Experimental Biology, 211, 2008, 3490-3503.
[22] A.A. Shirgaonkar, M.A. Maciver And N.A. Patankar, A New Mathematical Formulation And Fast Algorithm For Fully Resolved Simulation Of Self-Propulsion, Journal Of Computational Physics, 228, 2009, 2366-2390.
[23] I.D. Nevelin, R. Bale, A.P.S. Bhalla, O.M. Curet, N.A. Patankar And M.A. Maciver, Undulating Fins Produce Off-Axis Thrust And Flow Structures, Journal Of Experimental Biology, 217, 2014, 201-213.
[24] O.M. Curet, N.A. Patankar, G.V. Lauder And M.A. Maciver, Aquatic Maneuvering With Counter-Propagating Waves: A Novel Locomotive Strategy, Journal Of Royal Society: Interface, 1, 2010, Doi: 10.1098/Rsif.201 0.0493.
[25] M. Epstein, J.E. Colgate And M.A. Maciver, A Biologically Inspired Robotic Ribbon Fin, Proceeding Of The Ieee/Rsj International Conference On Intelligent Robots And Systems, Alberta, Canada, 2005, 1-6.
[26] M. Epstein, J.E. Colgate And M.A. Maciver, Generating Thrust With A Biologically-Inspired Robotic Ribbon-Fin, Proceeding Of The Ieee/Rsj International Conference On Intelligent Robots And Systems, Beijing, China, 2006, 1-7.
[27] M. Epstein, Generating Thrust With A Biologically-Inspired, Robotic Ribbon-Fin, Doctoral Diss., Northwestern University, Evanston, Il, 2006.
[28] M.B. Mehhaj, Computational Intelligence: Fundamental Of Neural Networks (Tehran: Amirkabir University Of Technology Publication, 2000).
[29] S. Haykin, Neural Networks: A Comprehensive Foundation (New Jersey: Prentice Hall, 1999).
[30] H. Mühlenbein, The Breeder Genetic Algorithm-A Provable Optimal Search Algorithm And Its Application, Ieee Colloquium On Applications Of Genetic Algorithms, London, Uk, 1994, 1-20.
[31] H. Mühlenbein And D. Schlierkamp-Voosen, Predictive Models For The Breeder Genetic Algorithm, Journal Of Evolutionary Computation, 1(1), 1993, 25-49.
[32] H. Mühlenbein And D. Schlierkamp-Voosen, The Science Of Breeding And Its Application To The Breeder Genetic Algorithm, Journal Of Evolutionary Computation, 1(4), 1993, 335-360.
[33] H. Mühlenbein And D. Schlierkamp-Voosen, Analysis Of Selection, Mutation And Recombination In Genetic Algorithms, Journal Of Neural Network World, 3, 1993, 907-933.